

Lattice distortion in a strain-compensated $\text{Si}_{1-x-y}\text{Ge}_x\text{C}_y$ layer on silicon

B. Dietrich, H.J. Osten, H. Rücker, M. Methfessel, and P. Zaumseil

Institute for Semiconductor Physics, P.O. Box 409, D-15204 Frankfurt (Oder), Germany

(Received 1 February 1994)

A number of $\text{Si}_{1-x-y}\text{Ge}_x\text{C}_y$ layers with different concentrations of Ge and C were grown by molecular-beam epitaxy on a Si(001) substrate to investigate the possibility of strain compensation. The layers were characterized by transmission electron microscopy, x-ray diffraction, and Raman scattering and modeled using a valence-force field model. For a $[\text{Ge}]/[\text{C}]$ ratio of approximately 10, the lattice constant in the growth direction is equal to that of the substrate, indicating the absence of macroscopic strain. Experimental and theoretical results are compatible with Vegard's rule. The bond lengths in the alloy exhibit a significant relaxation away from the ideal "chemical" value as given by the sum of the corresponding covalent radii. The measured shifts of the Raman frequencies relative to the constituents cannot be understood in a straightforward description based purely on the softening or hardening of the interatomic bonds as deduced from the Grüneisen parameters.

I. INTRODUCTION

Recently it was shown that small amounts of iso-electronic carbon added to a $\text{Si}_{1-x}\text{Ge}_x$ layer can provide an additional design parameter in manipulating the strain.^{1,2} The Si-C bond length is much smaller than the bond lengths in a $\text{Si}_{1-x}\text{Ge}_x$ alloy. Osten *et al.*³ exploited this to grow an inversely distorted lattice by adding 1.6% carbon to a $\text{Si}_{1-x}\text{Ge}_x$ layer with a germanium concentration of 10%. The tetragonal distortion of such a lattice is associated with tensile stress instead of the usual compressive stress present in pseudomorphic $\text{Si}_{1-x}\text{Ge}_x$ layers on silicon substrates. In such an inversely distorted system the distance of the lattice planes in the growth direction is smaller than in the interface plane, which equals the silicon lattice spacing for perfect pseudomorphy. One especially interesting feature in manipulating strain in pseudomorphic $\text{Si}_{1-x}\text{Ge}_x$ layers by adding carbon is the possibility of strain compensation to zero misfit. The perpendicular lattice constant of such a layer equals that of cubic silicon. Consequently the splitting in the valence band edge in a two-fold and four-fold degenerate valley observed for strained $\text{Si}_{1-x}\text{Ge}_x$ should disappear.

In general terms, a ternary Si-Ge-C alloy is quite different from $\text{Si}_{1-x}\text{Ge}_x$ because of the much shorter Si-C and Ge-C bond lengths, possibly leading to large lattice distortions near the carbon atoms. The microscopic arrangement of atoms in $\text{Si}_{1-x}\text{Ge}_x$, as measured in terms of the bond-length distributions, is still under debate. The two limiting cases⁴ are Pauling's model (in which each bond has a characteristic "chemical" length independent of the environment) and the "Vegard's rule" picture (in which all atoms lie on a perfect diamond lattice with an average lattice constant). A recent extended x-ray-absorption fine-structure (EXAFS) measurement⁵ supports the Pauling picture, whereas most theoretical approaches predict about 30% to 40% relaxation towards a common bond length.

In this paper we present the growth and characteri-

zation of a $\text{Si}_{1-x-y}\text{Ge}_x\text{C}_y$ layer on a Si(001) substrate which is almost strain compensated and shows the same perpendicular lattice constant as the silicon substrate. We will discuss the results of transmission electron microscopy (TEM), x-ray diffraction, and Raman spectroscopy on this sample. The measured samples were simulated using a modified valence-force (Keating) model which includes anharmonic effects. This permits a detailed analysis of the bond lengths in the strained alloys. The results confirm the previously predicted deviation from the ideal Pauling description. By comparing the calculated bond lengths in the various alloys with the measured phonon frequencies, we conclude that the phonon shifts upon alloying cannot be explained in a simple picture in which the bonds soften or harden in response to changes in their length.

II. EXPERIMENTAL RESULTS

The layers were grown in a solid source molecular-beam epitaxy (MBE) equipment using a pyrolytic graphite-filament sublimation cell as a solid carbon source. The used growth procedure has been described in detail in Ref. 3. Three samples with the intended compositions given in Table I were grown on a *p*-type Si(001) substrate following the deposition of an 80 nm thick *i*-Si buffer layer.

Osten *et al.*³ calculated the resulting misfit in a $\text{Si}_{1-x-y}\text{Ge}_x\text{C}_y/\text{Si}$ heterostructure assuming the validity of Vegard's law for both Ge and C alloying. The aver-

TABLE I. Composition of the prepared $\text{Si}_{1-x-y}\text{Ge}_x\text{C}_y$ layers.

Sample	Ge content x	C content y	Layer thickness
<i>a</i>	0.00	0.009	150 nm
<i>b</i>	0.11	0.009	200 nm
<i>c</i>	0.11	0.012	120 nm

age tetragonal deformation vanishes at a $[\text{Ge}]/[\text{C}]$ ratio of about 10. This result agrees very well with recent investigations by Im *et al.*⁶ These authors studied the strain-compensation effect by C atoms in solid phase epitaxy growth of $\text{Si}_{1-x}\text{Ge}_x$ alloy layers using sequential ion implantation. In our experiment the $[\text{Ge}]/[\text{C}]$ ratio was kept constant during the growth process by controlling the source temperature of the Ge effusion cell and the input power of the sublimation cell. The Ge content in sample *c* was measured as $x = 0.11$ after growth in an x-ray microanalyzer using the STRATA software.

The strain was measured in an x-ray double-crystal diffractometer (DCD) using $\text{Cu } K\alpha_1$ radiation and the symmetrical 400 reflection:

$$\epsilon_{\perp} = \frac{a_{\perp} - a_{\text{Si}}}{a_{\text{Si}}} \simeq -\frac{\Delta\Theta}{\tan \Theta_B}, \quad (1)$$

where ϵ_{\perp} and a_{\perp} are the strain and the lattice constant of the layer measured in a direction perpendicular to the sample surface, a_{Si} is the lattice parameter of the Si substrate, $\Delta\Theta$ the angular distance between the silicon substrate and the layer peak in the DCD rocking curve, and Θ_B the Bragg angle of the used reflection.

Figure 1 shows rocking curves of the three different samples with $\text{Si}_{1-y}\text{C}_y$ (curve *a*) and $\text{Si}_{1-x-y}\text{Ge}_x\text{C}_y$ (curves *b* and *c*) layers. The incorporation of carbon into the Si lattice results in a smaller lattice constant which leads to the occurrence of the layer peak at $\Delta\Theta > 0$ in the rocking curve *a* in Fig. 1. In the $\text{Si}_{1-x-y}\text{Ge}_x\text{C}_y$ system the effect of Ge to increase the average lattice

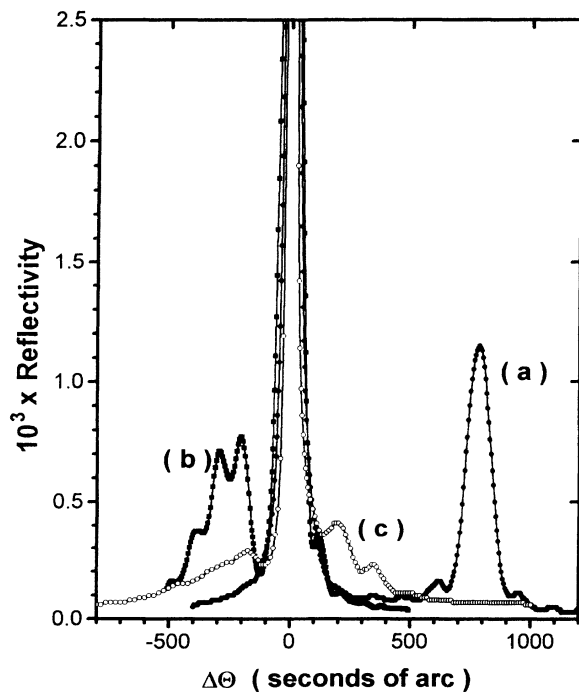


FIG. 1. Double crystal diffractometer rocking curve of three Si samples with embedded $\text{Si}_{1-y}\text{C}_y$ and $\text{Si}_{1-x-y}\text{Ge}_x\text{C}_y$ alloy layers measured using $\text{Cu } K\alpha_1$ radiation and the symmetrical 400-reflection: (a) 150 nm $\text{Si}_{0.99}\text{C}_{0.009}$; (b) 200 nm $\text{Si}_{0.881}\text{Ge}_{0.11}\text{C}_{0.009}$; (c) 120 nm $\text{Si}_{0.878}\text{Ge}_{0.11}\text{C}_{0.012}$.

constant can be compensated by carbon. Curve *b* in Fig. 1 shows a partial and curve *c* a nearly complete compensation of the strain. Additional triple-crystal diffractometer (TCD) measurements were performed to detect defect-related diffuse scattering. They indicate a good structural perfection of the samples. In comparison to a perfect Si substrate we did not find a significant difference in the amount of diffuse scattering. The x-ray diffraction correctly measures the lattice constant. This was derived by Härtwig and Holý⁷ from the dynamical theory of x-ray diffraction. The average is taken over a distance equal to the extinction length of x rays, which is of the order of micrometers.

The layers were also investigated in a transmission electron microscope (Philips CM 30) operating at 300 kV. Samples were prepared by chemical jet etching and ion milling. Both plan-view and cross-sectional TEM investigations (Fig. 2) indicate that the layer is free of dislocations and stacking faults. We also did not find any formation of precipitates.

Raman measurements were performed at room temperature in backscattering $z(x', y')\bar{z}$ geometry using a Dilor *xy* triple-grating spectrometer where x' is the crystallographic $[110]$ direction and y' is the $[\bar{1}10]$ direction. The microscopic entrance optics and a charge-coupled device (CCD) multichannel detector were used. The scattering was excited with the 457.9 nm and 514.5 nm lines of an Ar^+ ion laser. The laser power at the sample surface was less than 10^5 W/cm^2 . Overview spectra were measured in the subtractive mode. The line shift of the Si-Si Raman line was determined from measurements in the additive mode.

Supplementary Raman measurements were performed on cross-sectioned pieces of sample *c* in $y'(z, x')\bar{y}'$ and $y'(x', x')\bar{y}'$ geometries to examine the $\text{Si}_{1-x-y}\text{Ge}_x\text{C}_y$ layer for a tetragonal strain. The Si-Si mode would split in both scattering geometries under an existing biaxial strain.

A spectrum of the sample *c* is shown in Fig. 3. The strongest line at 520.5 cm^{-1} is the bulk Si mode. At 514.0 cm^{-1} the Si-Si mode of the layer appears. It is shifted to smaller wave numbers from the bulk silicon by 6.5 cm^{-1} due to the germanium content and perhaps to elastic strain, as is known for $\text{Si}_{1-x}\text{Ge}_x$ layers.⁸ The weaker peaks at 437, 407.4, and 287.2 cm^{-1} are the two

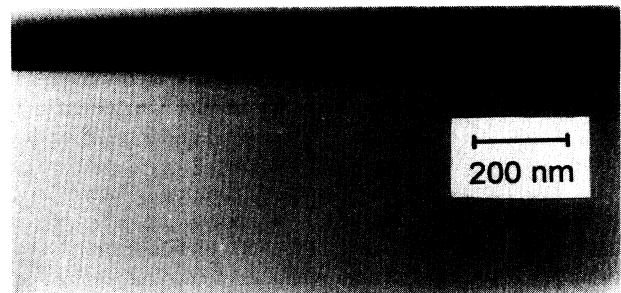


FIG. 2. Transmission electron micrograph of a cross-sectional cut through sample *c*. The silicon substrate is at the bottom. A thin marking line separates it from the silicon buffer layer in the middle. The $\text{Si}_{1-x-y}\text{Ge}_x\text{C}_y$ layer is seen on the top. It is darker due to the Ge content.

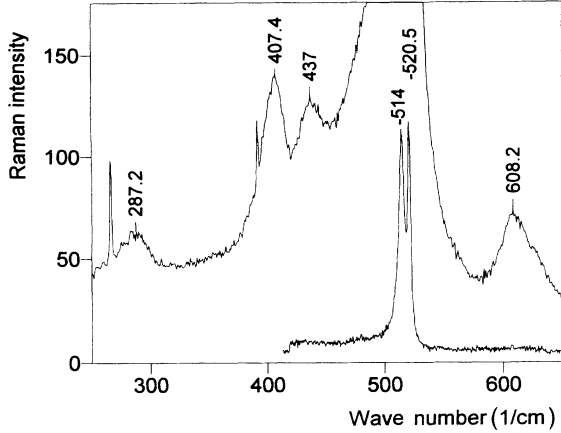


FIG. 3. Raman spectra of the $\text{Si}_{0.878}\text{Ge}_{0.11}\text{C}_{0.012}$ sample. The upper curve shows weak peaks at 287.2 cm^{-1} (Ge-Ge), at 407.4 and 437 cm^{-1} (Si-Ge), and the localized mode of the Si-C at 608.2 cm^{-1} . The bottom curve shows a high dispersion spectrum of the Si-Si modes in the substrate (520.5 cm^{-1}) and in the $\text{Si}_{1-x-y}\text{Ge}_x\text{C}_y$ layer (514.0 cm^{-1}). Intensity is plotted in arbitrary units.

Si-Ge and the Ge-Ge modes of the alloy. So far the spectrum corresponds well to known $\text{Si}_{1-x}\text{Ge}_x$ spectra for $x = 0.11$. The broad weak peak at 608.2 cm^{-1} is the localized ^{12}C - ^{28}Si mode overlapping the weak two-phonon peak of the p -type substrate. Furthermore, the broad low frequency wing of the bulk Si mode covering the 475 cm^{-1} region is caused by the C alloying. This spectrum corresponds well with the one published by Tsang *et al.*⁹ for a $\text{Si}_{1-x-y}\text{Ge}_x\text{C}_y$ layer with the exception that the localized C-Si mode is broader here and that an asymmetrical broadening occurs at 475 cm^{-1} .

The observed Raman line shift of the Si-Si mode in the strain-compensated $\text{Si}_{1-x-y}\text{Ge}_x\text{C}_y$ layer of sample *c* is given in Table II together with the corresponding line shifts of free-standing and pseudomorphically strained $\text{Si}_{1-x}\text{Ge}_x$ alloys with the same Ge content. The shift of the Si-Si mode in free-standing $\text{Si}_{1-x}\text{Ge}_x$ alloys is interpolated from the data of Alonso and Winer.¹⁰ Measured data for the dependence of the Si-Si mode in pseudomorphically strained SiGe alloys are summarized in Ref. 8. In a free-standing $\text{Si}_{0.89}\text{Ge}_{0.11}$ alloy the Si-Si mode is shifted by $\Delta\omega_{\text{alloy}} = -7.6\text{ cm}^{-1}$ against the Si-Si mode in the Si substrate.¹⁰ The pseudomorphic growth of the $\text{Si}_{0.89}\text{Ge}_{0.11}$ layer on a silicon substrate

generates a biaxial strain causing an additional strain-induced shift of $\Delta\omega_{\text{elast}} = +3.76\text{ cm}^{-1}$. The resulting total shift is $\Delta\omega_{\text{tot}} = -3.84\text{ cm}^{-1}$. The measured Raman shift $\Delta\omega = -6.5\text{ cm}^{-1}$ from the $\text{Si}_{0.878}\text{Ge}_{0.11}\text{C}_{0.012}$ layer is significantly larger than the value for the pseudomorphic layer and close to the value for the free-standing $\text{Si}_{1-x}\text{Ge}_x$ alloy. Furthermore, there is no significant difference between the measured Raman shifts in backscattering from faces parallel and perpendicular to the layer surface. This proves the absence of a tetragonal distortion in agreement with the x-ray measurements.

For the discussion below, we emphasize the comparison between the free-standing (strain-free) $\text{Si}_{0.89}\text{Ge}_{0.11}$ and $\text{Si}_{0.878}\text{Ge}_{0.11}\text{C}_{0.012}$ systems, whose Si-Si frequencies are shifted by, respectively, -7.6 and -6.5 cm^{-1} relative to the pure Si crystal. The measured frequency shifts were converted into those of the strain-free alloy using the relations given by Anastassakis.¹¹ Thus, the effect on the frequency when adding carbon is much smaller than for germanium, although the magnitudes of the change in crystal volume are the same.

III. CALCULATIONS

To study the elastic strain fields of $\text{Si}_{1-x-y}\text{Ge}_x\text{C}_y$ alloys, a valence-force field (Keating) model¹² is useful. The central property of the alloys considered here is the large inherent strain because the constituent atoms have very different sizes. We expect some bonds significantly stretched so that anharmonic effects become important. In order to describe anharmonic effects within the valence-force field model we have introduced a bond-length dependence of the interatomic force constants α and β . The strain energy¹²

$$E = \sum_{i,j} \alpha_{ij}(x_{ij}) \frac{3}{16r_{ij}^2} (x_{ij}^2 - r_{ij}^2)^2 + \sum_{i,j,k>j} \beta_{ijk}(x_{ij}, x_{ik}) \frac{3}{8r_{ij}r_{ik}} \left(\mathbf{x}_{ij}\mathbf{x}_{ik} + \frac{1}{3}r_{ij}r_{ik} \right)^2 \quad (2)$$

is modeled by the force constants α and β describing bond stretching and bond bending forces, respectively. The index i denotes the sum over all atoms with nearest neighbors $j, k = 1, \dots, 4$ and x_{ij} and r_{ij} are the strained and unstrained bond lengths, respectively. The parameters of the valence-force field model (Table III) were fitted to the results of *ab initio* total energy calculations for Si,

TABLE II. Raman shifts of the Si-Si mode in $\text{Si}_{1-x}\text{Ge}_x$ and $\text{Si}_{1-x-y}\text{Ge}_x\text{C}_y$ layers relative to the Si-Si mode in bulk silicon.

Scattering geometry	$\text{Si}_{0.89}\text{Ge}_{0.11}$ ^a strain-free	$\text{Si}_{0.89}\text{Ge}_{0.11}/\text{Si}$ ^b pseudomorphic	$\text{Si}_{0.878}\text{Ge}_{0.11}\text{C}_{0.012}$ ^c strain-free
$z(x', y')\bar{z}$	-7.60 cm^{-1}	-3.84 cm^{-1}	-6.50 cm^{-1}
$y'(z, x')\bar{y}'$	-7.60 cm^{-1}	-4.81 cm^{-1}	-6.52 cm^{-1}
$y'(x', x')\bar{y}'$	-7.60 cm^{-1}	-4.81 cm^{-1}	-6.94 cm^{-1}

^aIntrapolated from Ref. 10.

^bReference 8.

^cPresent measurements, sample *c*.

TABLE III. Atomic force constants for bond stretching and bond bending in diamond and zinc-blende structures of group IV elements in atomic units.

	Ge	SiGe	Si	GeC	SiC	C
α	0.050	0.053	0.061	0.096	0.114	0.192
β	0.015	0.016	0.018	0.033	0.038	0.109

Ge, C, and the zinc-blende phases of SiGe, SiC, and GeC under various strain conditions. From the calculation of the elastic constants for different lattice constants we have concluded that the bond stretching force constant α scales as x^{-4} whereas the bond bending force constant β scales as x^{-7} . The geometric mean of the bond bending force constants in the zinc-blende structures AB and AC is taken for those β_{ijk} where the sites i, j, k are occupied by atomic species A, B , and C , respectively. The details of the model will be presented elsewhere.¹³ All *ab initio* energies were obtained using the full-potential linear muffin-tin orbital method.¹⁴

The calculated bond-length distributions given by the model are shown in Fig. 4 for $\text{Si}_{0.988}\text{C}_{0.012}$, $\text{Si}_{0.89}\text{Ge}_{0.11}$, and $\text{Si}_{0.878}\text{Ge}_{0.11}\text{C}_{0.012}$ layers grown pseudomorphically on Si(001). The bond-length distribution was calculated by relaxing the atomic positions in a periodically repeated cluster of 2000 atoms with a random occupation of the lattice sites with Si, Ge, and C atoms and a subsequent averaging over twenty configurations. The $\text{Si}_{1-x}\text{Ge}_x$ alloy layer exhibits peaks at three characteristic bond lengths corresponding to the Si-Si, Si-Ge, and

Ge-Ge bonds. The average Si-Si bond length is close to the value of unstrained bulk Si. The lattice constant in the growth direction of the biaxially strained $\text{Si}_{0.89}\text{Ge}_{0.11}$ layer is $a_{\perp} = 1.0077a_{\text{Si}}$ where a_{Si} is the Si lattice constant. The smaller C atoms incorporated into the lattice of the pseudomorphous $\text{Si}_{0.988}\text{C}_{0.012}$ layer reduce the average volume of the alloy. Therefore the layer is biaxially strained and the lattice constant in the growth direction is reduced to $a_{\perp} = 0.9915a_{\text{Si}}$. The majority of Si-Si bonds in the $\text{Si}_{0.988}\text{C}_{0.012}$ alloy layer have a length close to the Si bulk value. The additional peaks appearing in the Si-Si bond-length distribution are related to bonds in the neighborhood of the C atoms. The Si-C bonds are stretched by about 7% with respect to the bond length in cubic SiC. The global strain is almost compensated in the $\text{Si}_{0.878}\text{Ge}_{0.11}\text{C}_{0.012}$ alloy layer as can be seen from the calculated lattice constant $a_{\perp} = 0.9992a_{\text{Si}}$. Local strain fields due to the incorporation of C broaden the Si-Si, Si-Ge, and Ge-Ge peaks by elongating bonds close to the C atoms. The calculated perpendicular lattice parameters of the considered $\text{Si}_{1-x-y}\text{Ge}_x\text{C}_y$ alloy layers are all in close agreement with the values obtained from Vegard's law in conjunction with the elastic theory.

IV. DISCUSSION

The experimental results and the valence-force field model are consistent in that both are in accord with Vegard's rule as applied to a mixture of Si, Ge, and C atoms. Our purpose is to use the model to supply detailed information about the atomic arrangement which is difficult to obtain experimentally. For example, we can determine the typical bond lengths between the different species in the alloy (Fig. 4). As has been discussed in Ref. 4, these are expected to lie between two limiting cases which are associated with Pauling and Vegard, respectively. In Pauling's picture, the bond length R_{AB} between atoms of species A and B is transferable and does not depend on the environment. In the second description, all atoms are assumed to lie on an ideal lattice. All bond lengths are then equal and the lattice constant comes out to the concentration-weighted average, giving a straightforward explanation of Vegard's rule. Note, however, that Pauling's picture is also consistent with a linear dependence of the lattice constant on the concentration. For a crystal $A_{1-x}B_x$ with the appropriate covalent radii r_A and r_B we obtain an average bond length

$$\begin{aligned} R_{\text{av}} &= (1-x)^2 R_{AA} + 2x(1-x)R_{AB} + x^2 R_{BB} \\ &= 2(1-x)r_A + 2xr_B, \end{aligned} \quad (3)$$

where the bond length R_{XY} equals $r_X + r_Y$ for each case $XY = AB, AA, \text{ or } BB$ and a stochastic distribution of A and B atoms was assumed.

A dimensionless constant ϵ expresses the degree of relaxation from the common "Vegard" bond length (case $\epsilon = 0$) towards Pauling's "chemical" values (for $\epsilon = 1$). Following Ref. 4 we take

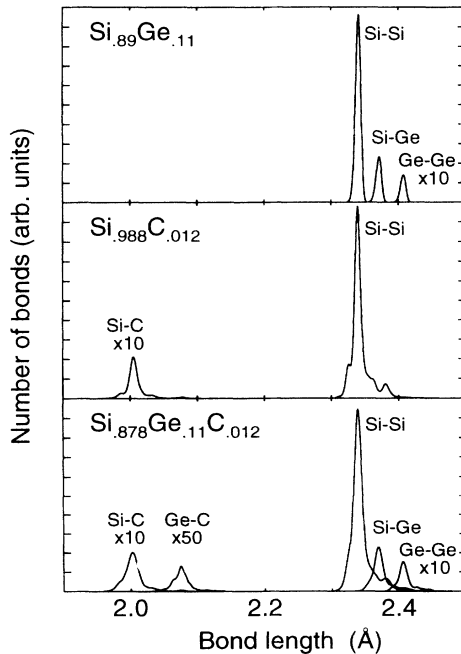


FIG. 4. Calculated bond-length distributions for $\text{Si}_{0.98}\text{Ge}_{0.11}$, $\text{Si}_{0.988}\text{C}_{0.012}$, and $\text{Si}_{0.878}\text{Ge}_{0.11}\text{C}_{0.012}$ layers pseudomorphically strained onto the Si(001) substrate. The curves of Si-C, Ge-Ge, and Ge-C were multiplied by factors of 10, 10, and 50, respectively.

$$\epsilon = \frac{R_{XY} - R_{av}}{R_{XY}^0 - R_{av}}, \quad (4)$$

where R_{av} is the average bond length of the alloy as given by Vegard's rule, R_{XY} is the observed characteristic bond length in the alloy, and R_{XY}^0 is the X - Y bond length in the ordered (zinc-blende or diamond structure) XY compound. For a binary alloy in which R_{XY} depends linearly on the B concentration x , the parameter ϵ is independent of x and is related to the slope by

$$\frac{dR_{XY}(x)}{dx} = (1 - \epsilon) \frac{dR_{av}}{dx} = (1 - \epsilon)(R_B^0 - R_A^0), \quad (5)$$

where R_A^0 and R_B^0 are the bond lengths in the pure A and B crystals. Figure 5 illustrates this for the $\text{Si}_{1-x}\text{Ge}_x$ alloy as obtained using the valence-force field model. We find that each characteristic bond length does in fact depend linearly on the concentration and obtain values of ϵ of 0.67, 0.68, and 0.68 for the Si-Si, Si-Ge, and Ge-Ge bonds, respectively. This is in disagreement with recent EXAFS measurements⁵ which essentially reproduce Pauling's picture for the considered Ge-Ge and Si-Ge bonds, that is, $\epsilon = 1$. In view of this discrepancy, it is useful that the Si-Ge system has been studied extensively in the framework of the *ab initio* pseudopotential method,¹⁵ giving ϵ values of 0.71, 0.72, and 0.70 for the three bond types. Given the well-known accuracy of the local-density method in calculating bond lengths, we tentatively assume that our valence-force field model describes the geometry of the alloy well, without speculating about the origin of the discrepancy with the EXAFS measurement.

This puts us into the position to consider the connection between the bond lengths in the alloy and the observed shifts of the phonon frequencies. In the following we consider the strain-free $\text{Si}_{1-x-y}\text{Ge}_x\text{C}_y$ alloys (see the end of Sec. II) to avoid complications due to biaxial distortion. It is well known that the Si-Si mode is softened

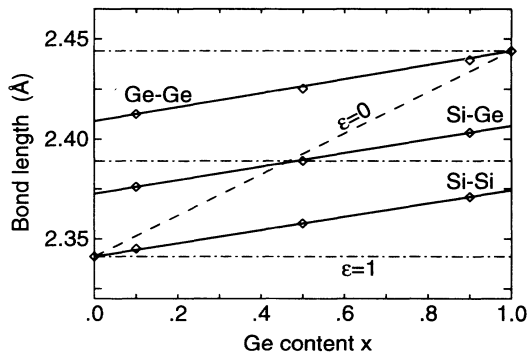


FIG. 5. Variation of the Si-Si, Si-Ge, and Ge-Ge bond lengths (full lines) in a $\text{Si}_{1-x}\text{Ge}_x$ alloy as function of the germanium content as calculated with the valence-force field model (diamonds). The dashed line corresponds to the “Vegard” limit of a common ideal lattice; the dash-dotted lines correspond to Pauling’s picture of transferable “chemical” bond lengths.

substantially when Ge is added to the crystal.^{10,16} The most interesting point in the present result is that further addition of C to such an alloy does not cause a significant additional shift of the Si-Si frequency despite the change in crystal volume. The success of the Keating model in describing semiconductors shows that lattice dynamics can be understood in term of short-range force constants. For the optical Γ mode, the bond stretching force constant α dominates. This becomes softer when the equilibrium bond length is increased and harder when it is reduced as described by the Grüneisen parameter. While this is clearly an important ingredient to understand the phonon shifts upon alloying, the comparison of experiment and theory shows that further effects must be taken into account. The simplest possible model, estimating the shift from the average alloy lattice constant, can in fact reproduce⁸ the Si-Si frequency in $\text{Si}_{1-x}\text{Ge}_x$ but contradicts the analogous softening¹⁰ of the Ge-Ge mode when the Si content is increased. It also fails for the phonon shift when C is added to the Si-Ge alloy; while the volume is reduced back to the silicon value, the frequency shift due to germanium is *not* compensated. In any case, this simple description is doubtful since it implicitly is based on the “Vegard” limit for the alloy bond lengths, which has been shown to be invalid by theory as well as by experiment.⁵

A more sophisticated description could estimate the phonon shifts in a similar manner, but deduces the bond softening or hardening from the calculated realistic bond lengths. In a real crystal, bond lengths relax towards the “Vegard” limit to some extent, but still lie closer to the “chemical” value. Therefore, adding Si to a Ge crystal shortens the Ge-Ge bond, albeit by a smaller amount than in the “Vegard” description. This means that the Grüneisen estimate still gives the wrong sign of the Ge-Ge mode shift even if a realistic bond-length behavior is introduced. On the other hand, this approach cannot reproduce the phonon shift when carbon is added, either. By direct inspection of the calculated bond-length distributions, we find that the Si-Si distance equals that of pure silicon for the strain-compensated $\text{Si}_{1-x-y}\text{Ge}_x\text{C}_y$ alloy whereas it is larger by 0.15% for $\text{Si}_{0.89}\text{Ge}_{0.11}$. The Grüneisen estimate consequently predicts incorrect shifts of zero and -2.3 cm^{-1} , respectively. From this we conclude that a simple description based on the softening via the Grüneisen parameter describes only one contribution to the phonon shift and that further effects must be included.

V. SUMMARY AND CONCLUSIONS

A strain-free $\text{Si}_{1-x-y}\text{Ge}_x\text{C}_y$ layer was grown on Si(001) by choosing the concentrations x, y such that the volume changes due to the germanium and carbon atoms compensate. This case was obtained for $x = 0.11$ and a value of y estimated to be about one-tenth of the germanium concentration, in agreement with Vegard’s rule. By comparing the measured Raman frequencies with the atomic arrangement obtained from a valence-force field model,

the connection between the phonon shifts and the interatomic bond-lengths was investigated. This showed that it is not possible to interpret the frequencies by translating the bond-length distortions into phonon shifts via the Grüneisen parameter.

ACKNOWLEDGMENTS

The authors would like to thank E. Bugiel for the TEM investigations and M. Kittler for the x-ray microanalyzer results.

-
- ¹ K. Eberl, S. S. Iyer, S. Zollner, J. C. Tsang, and F. K. LeGoues, *Appl. Phys. Lett.* **60**, 3033 (1992).
- ² A. R. Powell, K. Eberl, B. A. Ek, and S. S. Iyer, *J. Cryst. Growth* **127**, 425 (1993).
- ³ H. J. Osten, E. Bugiel, and P. Zaumseil, *Appl. Phys. Lett.* (to be published).
- ⁴ J. L. Martins and A. Zunger, *Phys. Rev. B* **30**, 6217 (1984).
- ⁵ H. Kajiyama, S. Muramatsu, T. Shimada, and Y. Nishino, *Phys. Rev. B* **45**, 14 005 (1992).
- ⁶ S. Im, J. Washburn, R. Gronsky, N. W. Cheung, K. M. Yu, and J. W. Ager, *Appl. Phys. Lett.* **63**, 2682 (1993).
- ⁷ J. Härtwig and V. Holý, *Phys. Status Solidi B* **135**, 37 (1986).
- ⁸ B. Dietrich, E. Bugiel, J. Klatt, G. Lippert, T. Morgenstern, H. J. Osten, and P. Zaumseil, *J. Appl. Phys.* **74**, 3177 (1993).
- ⁹ J. C. Tsang, K. Eberl, S. Zollner, and S. S. Iyer, *Appl. Phys. Lett.* **61**, 961 (1993).
- ¹⁰ M. I. Alonso and K. Winer, *Phys. Rev. B* **39**, 10 056 (1989).
- ¹¹ E. Anastassakis, *ESSDERC 89, Proceedings of the Sat. Symposium on Analytical Techniques for Semiconductor Materials and Process Characterization*, edited by B. O. Kolbesen (The Electrochemical Society, Pennington, 1990), p. 298.
- ¹² P. N. Keating, *Phys. Rev.* **145**, 637 (1966).
- ¹³ H. Rücker and M. Methfessel (unpublished).
- ¹⁴ M. Methfessel, C. O. Rodriguez, and O. K. Andersen, *Phys. Rev. B* **40**, 2009 (1989).
- ¹⁵ S. de Gironcoli, P. Giannozzi, and S. Baroni, *Phys. Rev. Lett.* **66**, 2116 (1991).
- ¹⁶ S. de Gironcoli, *Phys. Rev. B* **46**, 2412 (1992).

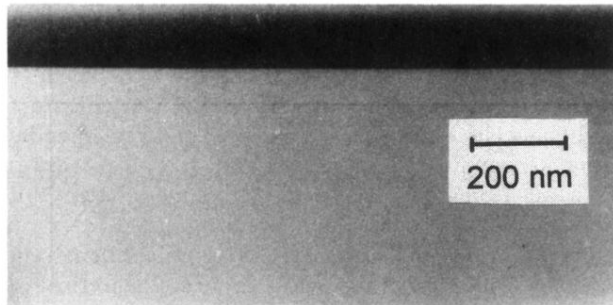


FIG. 2. Transmission electron micrograph of a cross-sectional cut through sample *c*. The silicon substrate is at the bottom. A thin marking line separates it from the silicon buffer layer in the middle. The $\text{Si}_{1-x-y}\text{Ge}_x\text{C}_y$ layer is seen on the top. It is darker due to the Ge content.